Supporting Information

General Fabrication of 3D Hierarchically Structured Bamboo-Like Nitrogen-Doped Carbon Nanotube Arrays on 1D Nitrogen-Doped Carbon Skeletons for Highly Efficient Electromagnetic Wave Energy Attenuation

Yuping Wang,† Bing Suo,† Yanan Shi,† Haoran Yuan,† Chunling Zhu,*,‡ and Yujin Chen*,†

† Key Laboratory of In-Fiber Integrated Optics, and College of Physics and Optoelectronic Engineering, Harbin Engineering University, Harbin 150001, China.

‡ College of Material Science and Chemical Engineering, Harbin Engineering University, Harbin 150001, China.

Corresponding Authors

E-mail addresses: chenyujin@hrbeu.edu.cn (Y. C.) or zhuchunling@hrbeu.edu.cn (C. Z.)

EXPERIMETNAL SECTION

Materials. Ethanol and dicyandiamide (DCDA) were purchased from Tianjin Guangfu Fine Chemical Research Institute (China). Isopropyl alcohol (IPA) was purchased from Tianjin Fuyu Fine Chemical Research Institute (China). $CoCl_2 \cdot 6H_2O$ was purchased from Tianjin in Basifu Chemical Reagent Co., Ltd (China). $NiCl_2 \cdot 6H_2O$ and nitrilotriacetic acid (NTA) was purchased from Sinopharm Chemical Reagent Co. Ltd. $FeCl_2 \cdot 4H_2O$ was purchased from Alfa Aesar. All materials were purchased without further treatment. All aqueous solutions were prepared using ultrapure water (>18 $M\Omega$).

Preparation of precursors nanowires. According to the reported literature, precursor nanowires were synthesized by solvothermal method.[28] For Fe-precursor nanowires, 1.25 g of $FeCl_2 \cdot 4H_2O$ and 600 mg of NTA were added to the mixed solution containing 13 mL of H_2O and 27 mL of IPA. After being stirred for vigorously several minutes, the mixture was transferred to Teflon container (50 mL), and then reacted at 180 °C for 6 h. After being cooled naturally, the precipitate was collected by centrifugation, and then washed with ultrapure water and ethanol.

Co- and Ni-precursor nanowires were synthesized through the same processes mentioned above except that $FeCl_2 \cdot 4H_2O$ was replaced with $CoCl_2 \cdot 6H_2O$ and $NiCl_2 \cdot 6H_2O$, respectively.

Synthesis of HMCNT. Two ceramic boats with the 50 mg of the M-precursors nanowires and 1.0 g of DCDA were placed in a tube furnace. The ceramic boat with DCDA was placed at the upstream side of the furnace. Under an Ar flow, the tube furnace was heated to 800 °C with a rate of 2 °C•min^{-1} for 2 h.

Characterizations. X-ray diffraction (XRD) was conducted on a X'Pert Pro diffractometer with Cu Kα radiation (λ=1.5418Å). Scanning electron microscopy (SEM) images were taken using a HITACHI SU8000 operating at 10 keV. Transmission electron microscopy (TEM) images were performed on a JEM-2100F transmission electron microscope. X-ray photoelectron spectroscopy (XPS) analyses were carried out by using a spectrometer with Al Kα radiation (1486.6eV PHI 5700 ESCA System). Raman spectra were recorded on a Raman spectrometer (Lab RAMA ramis, Horiba Jobin Yvon) using a 488 nm He-Ne laser. Brunauer-Emmett-Teller (BET) surface area and pore volume were tested with a Quantachrome Instruments NOVA4000. Thermogravimetry (TG) curve in air at the temperature of $0 - 800$°C was measured by a TA instruments-Waters LLC TG thermal gravimetric analyzer with a ramping rate of 10°C·min^{-1}. The magnetic property of the samples was measured by a vibrating sample magnetometer (VSM; Lakeshore 7410). The absorbance of HMCNTs was examined by UV-Vis spectrophotometer (UV-2450, Shimadzu).The chemical composition of the samples was determined by inductively coupled plasma-optical emission spectroscopy (ICP-OES) were tested by Optima 8000PE.

Electromagnetic parameter measurements. The electromagnetic parameters of the HMCNTs were measured using a vector network analyzer (Anritsu MS4644A Vectorstar). The tested cylindrical sample (3.04 mm in inner diameter and 7.00 mm in outer diameter) was prepared by mixing HMCNTs with paraffin matrix with a weight percentage of 15 wt%, 17 wt%, and 20 wt% for HNiCNT, HFeCNT, and HCoCNT, respectively.
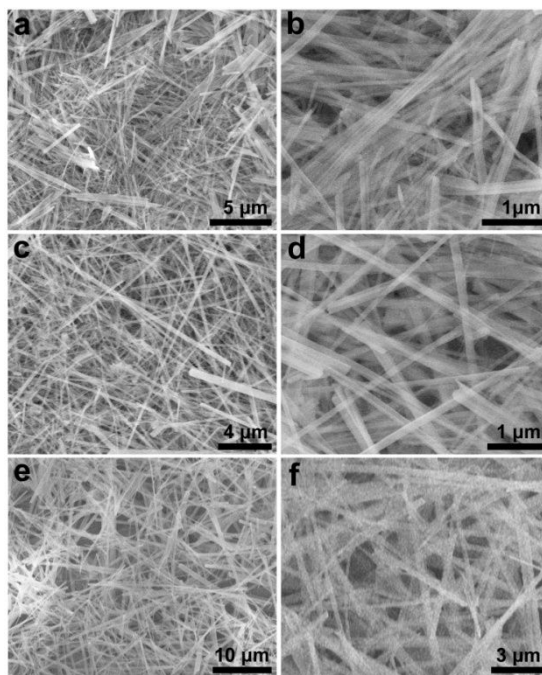

Figure S1 SEM images of a, b) Fe-precursor nanowires, c, d) Co-precursor nanowires, and e, f) Ni-precursor nanowires.
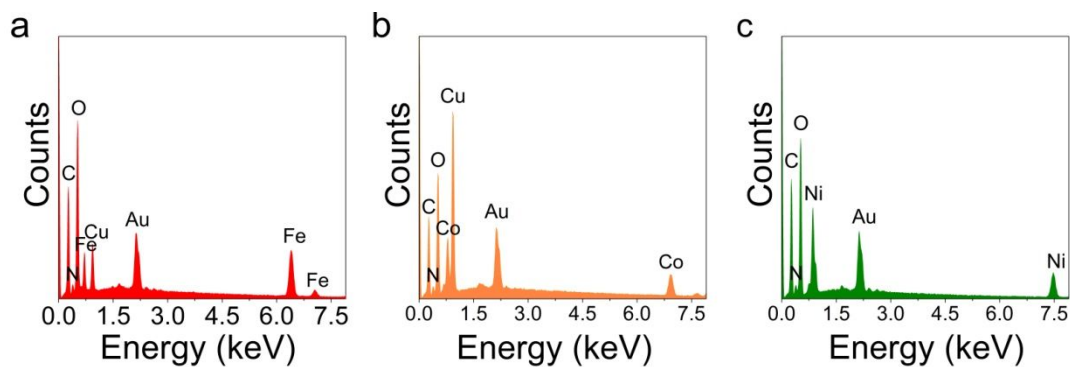

Figure S2 EDX patterns of a) Fe-precursors nanowires, b) Co-precursors nanowires, and c) Ni-precursors nanowires. (The Cu and Au elements were derived from supporter of copper plate and spray-gold.).
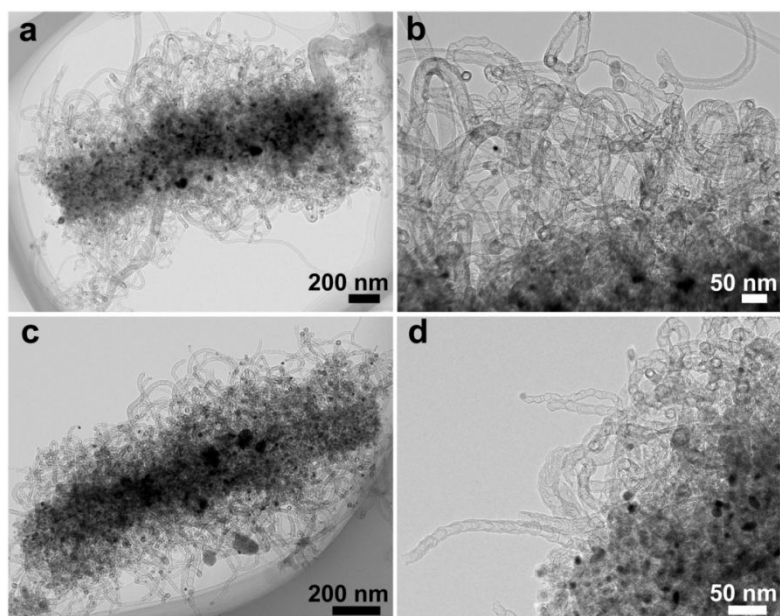
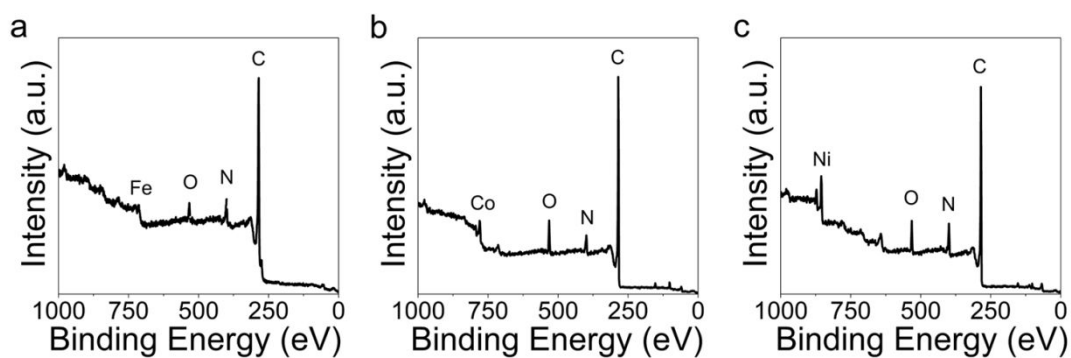**Figure S3** TEM images of a, b) HCoCNT and c, d) HNiCNT.

Figure S4 The survey XPS spectrums of a) HFeCNT, b) HCoCNT, and c) HNiCNT.
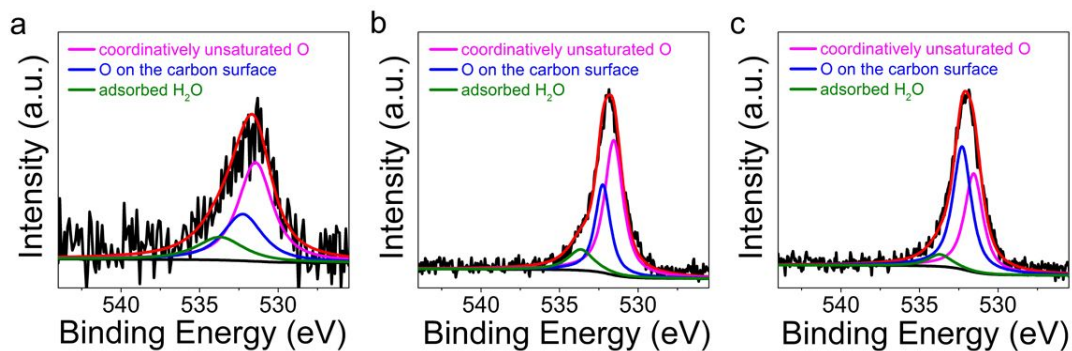

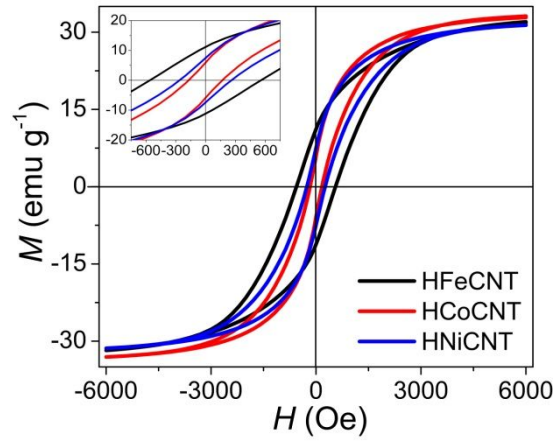**Figure S5** The O 1s core level XPS spectra of a) HFeCNT, b) HCoCNT, and c) HNiCNT.

Figure S6 Magnetization hysteresis loops of HMCNTs. The inset shows an enlarged image.
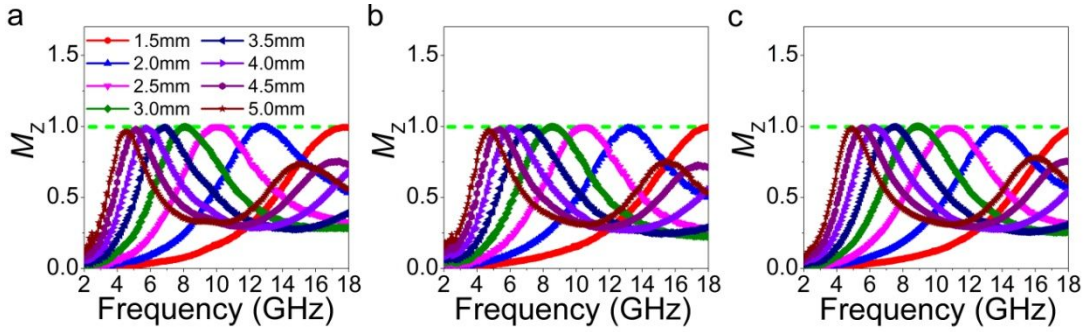

Figure S7 The $M_Z - f$ curves of a) HFeCNT, b) HCoCNT, and c) HNiCNT in the frequency range of $2 - 18$ GHz.
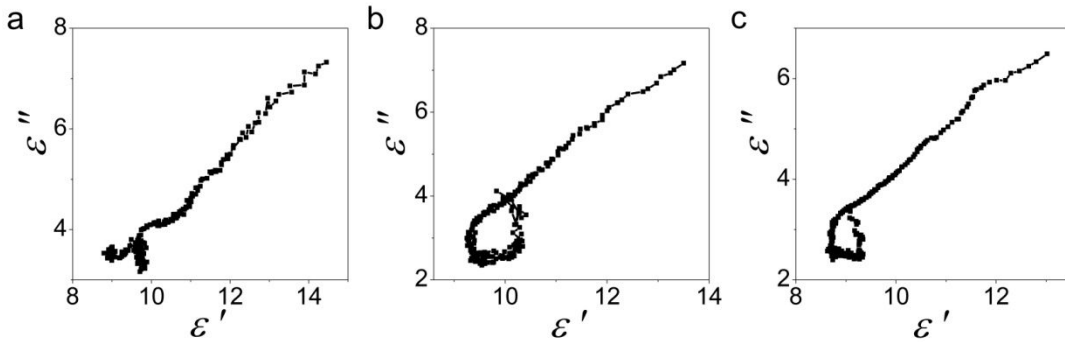

Figure S8 Typical Cole $-$ Cole semicircles (ε'' vs ε') for a) HFeCNT, b) HCoCNT, and c) HNiCNT.
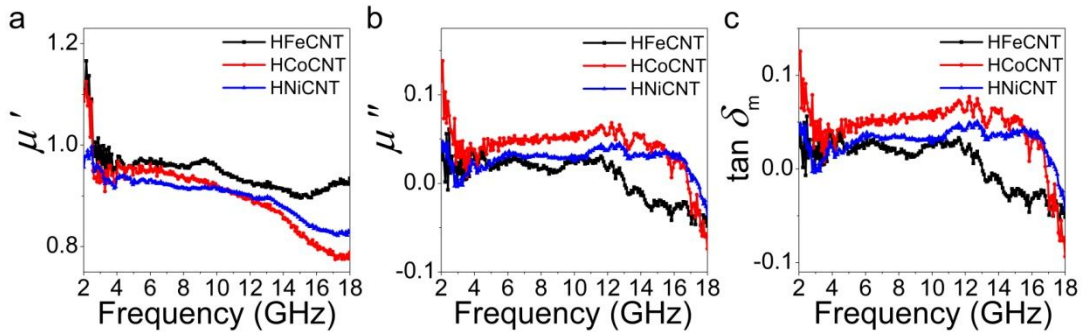

Figure S9 a) Real parts, b) imaginary parts of the relative complex permeabilities, and c) magnetic loss tangents of the HMCNTs.
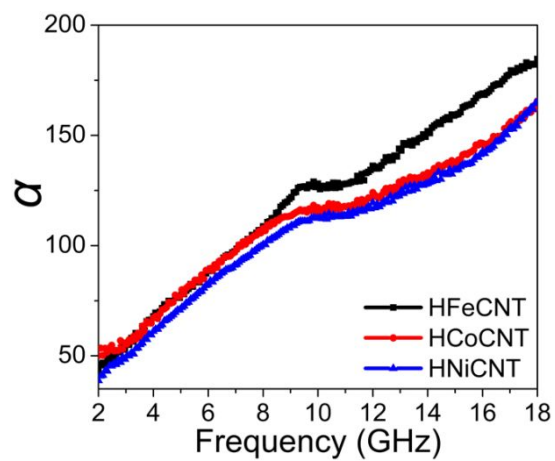
Figure S10 The attenuation constant α data of the HMCNTs.

Figure S11 The UV–Vis absorption spectra of HMCNTs.

Figure S12 a) SEM images and b) the enlarged detail of the HFeCNT obtained at 700 ^{o}C.
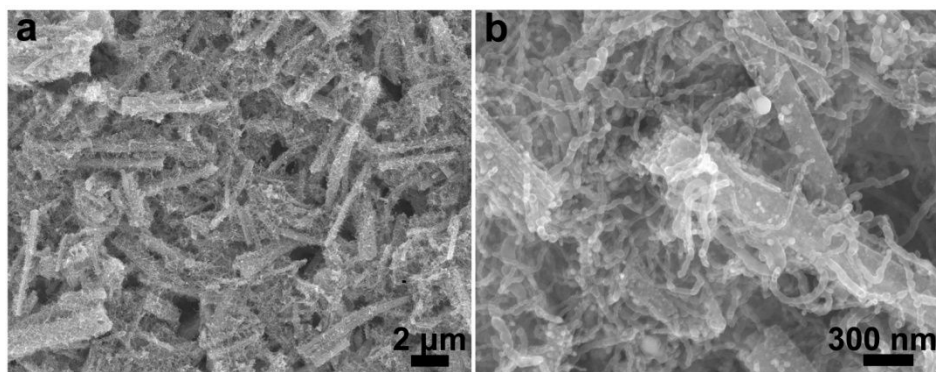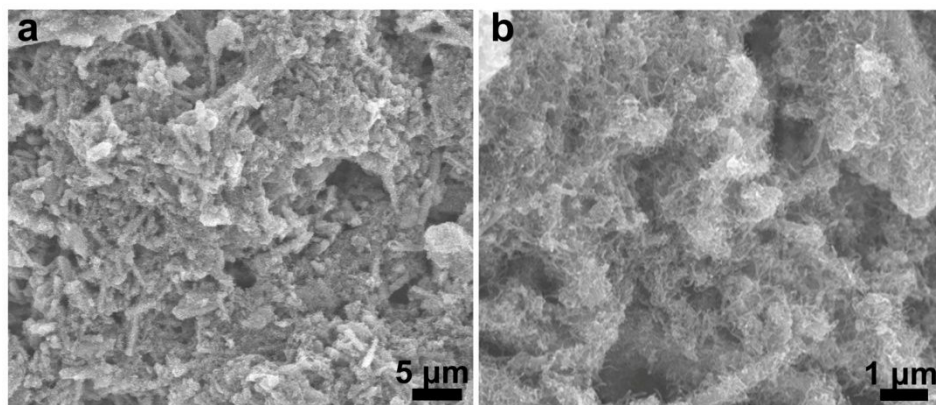
Figure S13 a) SEM images and b) the enlarged detail of the HFeCNT obtained at 900 °C.
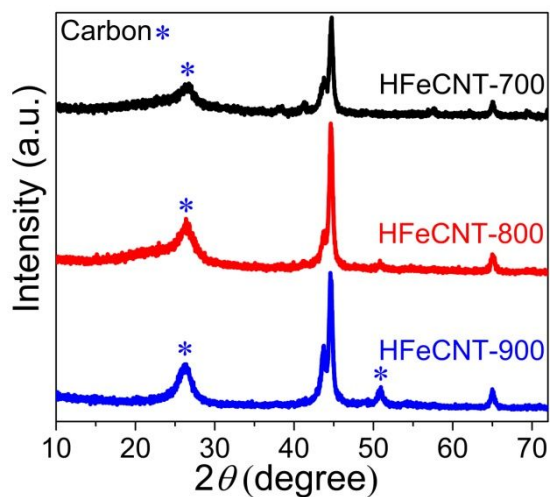

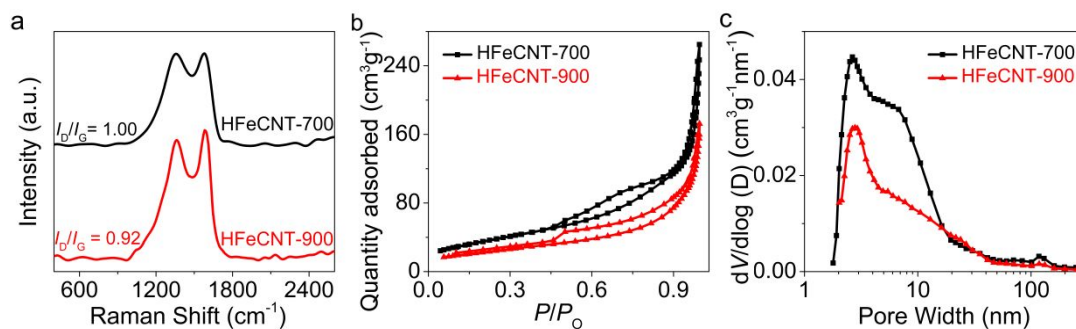**Figure S14** XRD patterns of the HFeCNTs obtained at 700, 800 and 900 °C.

Figure S15 a) Raman spectras, b) N_2 absorption/desorption isotherms, and c) pore size distribution curves of the HFeCNTs obtained at 700 and 900 °C.
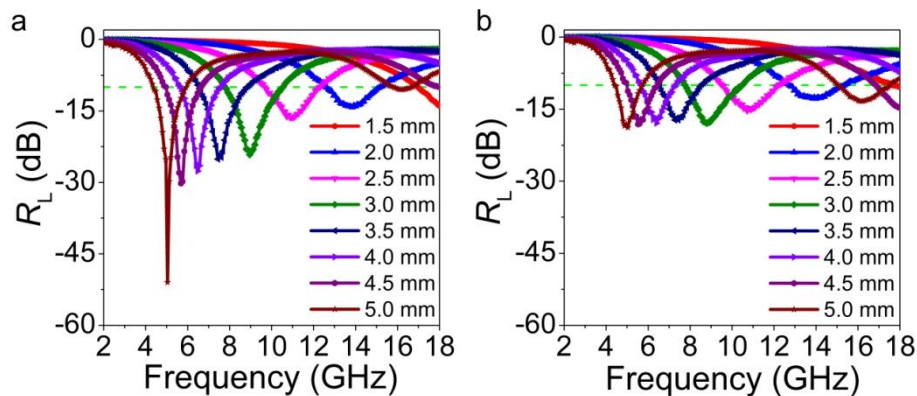
Figure S16 The $R_L - f$ curves of the a) HFeCNT obtained at 700 °C and b) HFeCNT obtained at 900°C in the frequency range of $2 - 18$ GHz.

Table S1 Elemental compositions of the HMCNTs.

Samples	Elements	ICP–OES (wt%)	TGA (wt%)
HFeCNT	Fe	23.68	23.72
HCoCNT	Co	28.27	28.34
HNiCNT	Ni	26.60	26.65

Table S2 Detail comparison of the EMW absorption property of the HMCNTs to others.

Sample	$R_{L\ min}$ (dB)	$EAB_{f=10}$ (GHz)	Thickness (mm)	Ref
3D MWNTs@PS	−34.2	3.0	−	16
CNTs@TiO$_2$ sponge	−31.8	2.8	2.0	26
Fe$_3$O$_4$/CNTs	−51.3	3.9	4.4	27
Fe$_3$O$_4$@C	−29.0	5.0	5.0	60
CNT@Fe@SiO$_2$	−22.3	3.5	3.0	S1
ZnO$_{nws}$/RGO foam/PDMS composite	−27.8	4.2	4.8	S2
PVDF/RGO	−25.6	3.3	4.0	S3
FeCo/C	−29.0	3.1	4.0	S4
MWCNT/Fe$_3$O$_4$ nanohybrid	−41.6	1.5	3.4	S5
GO/CNT-Fe$_3$O$_4$ nanohybrid	−37.2	1.0	5.0	S6
Fe$_x$C$_y$N$_z$/N-CNT	−25.1	1.3	4.0	S7

Sample				
Fe/Fe$_3$C@NCNTs-600	−46.0	1.2	4.97	S8
Co/N-C NFs	−25.7	4.3	2.0	S9
HFeCNT	−41.9	3.6	2.5	This work
HCoCNT	−31.9	2.1	2.5	This work
HNiCNT	−36.4	3.2	3.0	This work

Table S3 The EAB and $R_{L,m}$ of the HFeCNT obtained at 700, 800 and 900 ℃ at low matching thicknesses.

Sample	R_L (dB)	EAB (GHz)	Low Matching Thicknesses (mm)
HFeCNT 700 ℃	− 51.0	1.6	5.0
HFeCNT 800 ℃	− 41.9	3.1	2.5
HFeCNT 900 ℃	− 18.8	3.8	5.0

References

(1) Lv, H. L.; Ji, G. B.; Zhang, H. Q.; Du, Y. W. Facile Synthesis of a CNT@Fe@SiO$_2$ Ternary Composite with Enhanced Microwave Absorption Performance. *RSC Adv*. **2015**, *5*, 76836-76843.

(2) Song, C. Q.; Yin, X. W.; Han, M. K.; Li, X. L.; Hou, Z. X.; Zhang, L. T.; Cheng, L. F. Three-Dimensional Reduced Graphene Oxide Foam Modified with ZnO Nanowires for Enhanced Microwave Absorption Properties. *Carbon* **2017**, *116* , 50-58.

(3) Zhang, X. J.; Wang, G. S.; Cao, W. Q.; Wei, Y. Z.; Cao, M. S.; Guo, L. Fabrication of Multi-Functional PVDF/RGO Composites via a Simple Thermal Reduction Process and Their Enhanced Electromagnetic Wave Absorption and Dielectric Properties. *RSC Adv*. **2014**, *4*, 19594-19601.

(4) Han, Z.; Li, D.; Wang, H.; Liu, X. G.; Li, J.; Geng, D. Y.; Zhang, Z. D. Broadband Electromagnetic-Wave Absorption

by FeCo/C Nanocapsules. *Appl. Phys. Lett.* **2009**, *95,* 023114.

(5) Wang, Z. J.; Wu, L. N.; Zhou, J. G.; Cai, W.; Shen, B. Z.; Jiang, Z. H. Magnetite Nanocrystals on Multiwalled Carbon Nanotubes as a Synergistic Microwave Absorber. *J. Phys. Chem. C* **2013**, *117*, 5446-5452.

(6) Wang, L. N.; Jia, X. L.; Li, Y. F.; Yang, F.; Zhang, L. Q.; Liu, L. P.; Ren, X.; Yang, H. T. Synthesis and Microwave Absorption Property of Flexible Magnetic Film Based on Graphene Oxide/Carbon Nanotubes and Fe_3O_4 Nanoparticles. *J. Mater. Chem. A* **2014**, *2*, 14940-14946.

(7) Zhou, Y. L.; Miao, J.; Shen, Y. H.; Xie, A. J. Novel Porous $Fe_xC_yN_z$/N-Doped CNT Nanocomposites with Excellent Bifunctions for Catalyzing Oxygen Reduction Reaction and Absorbing Electromagnetic Wave. *Appl. Surf. Sci.* **2018**, *453*, 83-92.

(8) Xu, Z.; Du, Y. C.; Liu, D. W.; Wang, Y. H.; Ma, W. J.; Wang, Y.; Xu, P.; Han, X. J. Pea-Like Fe/Fe_3C Nanoparticles Embedded in Nitrogen-Doped Carbon Nanotubes with Tunable Dielectric/Magnetic Loss and Efficient Electromagnetic Absorption. *ACS Appl. Mater. Interfaces* **2019**, *11*, 4268-4277.

(9) Liu, H. H.; Li, Y. J.; Yuan, M. W.; Sun, G. B.; Li, H. F.; Ma, S. L.; Liao, Q. L.; Zhang, Y. In Situ Preparation of Cobalt Nanoparticles Decorated in N-DopedCarbon Nanofibers as Excellent Electromagnetic Wave Absorbers. *ACS Appl. Mater. Interfaces* **2018**, *10*, 22591-22601.